Journal of Computational Electronics (2020) 19:792–799
https://doi.org/10.1007/s10825-020-01482-w

Interplay between channel and shot noise at the onset of spiking activity in neural membranes

Beatriz G. Vasallo[1] · **Javier Mateos**[1] · **Tomás González**[1]

Published online: 12 March 2020

Abstract
The role played by ion channel noise and ion shot noise around the threshold conditions for spiking activity in biological membranes is studied by means of a stochastic model based on the Hodgkin–Huxley equations, considering membrane voltage-dependent gating channels for sodium and potassium cations, and leakage channels. Ion channel noise, that is, the noise linked to the random opening and closing of the ion channels, is included by means of Langevin sources. Ion shot noise, associated with the random passage of ions through the cell membrane, is considered by using the Gillespie's method, in terms of the probabilities for different ions to cross the membrane. The threshold for spiking activity is reached by applying increasing values of an external excitation I_{app} in a large membrane patch S, for which the strength of channel noise is insufficient for the onset of spikes in the absence of I_{app}. On the other hand, since by decreasing S the strength of both noise sources increases, spiking activity is also achieved for small enough values of S when $I_{app}=0$. The noise behavior of this biological system is analyzed in terms of the autocorrelation function and the spectral density of the membrane voltage fluctuations. Even if ion shot noise is typically considered as negligible when other electrical sources of neural noise are taken into account, the results indicate that, particularly around the onset of instabilities, the signature of shot noise, by the interplay with channel noise, is evident in the spectral density of the membrane voltage fluctuations.

Keywords Ion shot noise · Ion channel noise · Hodgkin–Huxley equations · Cell membrane

1 Introduction

The development of bioinspired electronic devices and circuits mimicking the brain functionality is of increasing interest both for low-power applications and for the further comprehension of the human brain [1–5]. In this context, the study of the noise behavior in biological membranes is compulsory since it can trigger the neuronal spiking activity [6–8]. The time evolution of electrical quantities in cell membranes, essential to explain the physical properties of neurons and axons [9, 10], is typically modeled by means of the phenomenological Hodgkin–Huxley (HH) equations [11]. This model accounts for the equilibrium conditions and the so-called action potential, which is a spike appearing in the voltage between the inside and the outside regions of cell membrane V_m activated by sufficient excitation with an external current density I_{app}. As nonlinear systems that evolve from a threshold, the analysis of their subthreshold regime, in particular the role played by noise, is especially relevant [12–14].

The main goal of the present analysis is the comprehension of the role played by both channel noise and shot noise on the spiking activity in cell membranes, particularly at the onset of instabilities. In our approach, ion channel assemblies are described as a whole by means of a continuous model [15–19]. The presence of ion channel noise, i.e., the noise related to the random opening and closing of the ion gates through the membrane, is taken into account by considering the Langevin generalization for the HH equations [15]. Ion shot noise, which is the noise associated with the random passage of ions across the cell membrane, is included by using the Gillespie's method, from the probabilities for ions to pass through the membrane [16–19]. Firstly, the noise behavior is studied for membrane patches S sufficiently large, so that channel noise and shot noise are insufficient for the onset of voltage spikes in the absence of external excitation. The threshold for spiking activity is

✉ Beatriz G. Vasallo
bgvasallo@usal.es

[1] Dpto. Física Aplicada, Universidad de Salamanca, Plaza de la Merced s/n, 37008 Salamanca, Spain

reached by applying increasing values of I_{app}. Secondly, the analysis is performed for decreasing values of S while keeping $I_{app}=0$. In that case, the conditions for the onset of instabilities are achieved just by reducing S, since the strength of both noise sources is enhanced, resulting in an increasing number of spontaneous spikes. The noise performance of the system is evaluated in terms of the autocorrelation function $C_{V_m}(t)$ and the spectral density $S_{V_m}(f)$ of the membrane voltage fluctuations.

The present work is organized as follows. In Section 2, the employed physical model is detailed. Our main results are explained in Section 3, and, afterward, the most important conclusions of this work are drawn in Section 4. Even if ion shot noise has been typically considered as negligible as compared to other electrical sources of neural noise [6, 15, 20–23], according to our results, the signature of shot noise becomes visible predominantly in the limits of subthreshold conditions by virtue of the interplay with channel noise.

2 Physical model

The cell membrane can be considered as an insulator separating the intracellular and the extracellular regions, which are electrolytes containing sodium and potassium cations, Na^+ and K^+. Ion leakage and voltage-gated channels for Na^+ and K^+ ions connect the inside and the outside regions through the membrane. According to the HH model [11], the electrical evolution of the cell membrane is described in time domain in terms of the membrane voltage $V_m(t)$, linked to the amount of charge at each side of it, and therefore to the ion currents crossing the membrane and the so-called gating variables: $m(t)$, $h(t)$ and $n(t)$, which determine the opening or the closing of sodium and potassium channels. In our model, the equations are solved in time domain by means of the standard Euler algorithm with a time step $\Delta t=2$ μs [15–19]. At every Δt, a new value of V_m is evaluated as

$$C_m \frac{dV_m(t)}{dt} = I_{app} - \sum_{ion} I_{ion}, \tag{1}$$

where C_m is the membrane capacitance per unit surface and I_{app} is an external excitation current density (here, considered as noiseless), which can initiate a voltage spike. I_{ion}, with the subindex ion = Na, K or leak, is the current density due to sodium cations, potassium cations or ion leakage, respectively.

In the HH deterministic model, the ion currents I_{ion}^{HH} are described in terms of channel conductances as:

$$I_{Na}^{HH}(V_m) = g_{Na}(V_m)(V_m - V_{Na}), \tag{2}$$

$$I_K^{HH}(V_m) = g_K(V_m)(V_m - V_K), \tag{3}$$

$$I_{leak}^{HH}(V_m) = g_{leak}(V_m - V_{leak}), \tag{4}$$

where g_{ion} are the gated conductances and V_{ion} are the so-called reversal potentials (at which the ion currents change their sign). g_{Na} depends on the dimensionless gating parameters $m(t)$ and $h(t)$ as [11]

$$g_{Na}(V_m) = g_{Na}^{max} m^3(t) h(t), \tag{5}$$

where g_{Na}^{max} is the maximal sodium conductance. $m(t)$ and $h(t)$ can be interpreted as the fraction of activation or inactivation molecules in the open state. Sodium cations can move through the membrane if three activation molecules are in their open state and one inactivation molecule is in its non-blocking state [11]. g_K depends on the dimensionless gating parameter $n(t)$ as

$$g_K(V_m) = g_K^{max} n^4(t), \tag{6}$$

where g_K^{max} is the maximal potassium conductance. $n(t)$ is related to the proportion of activation molecules in the open state. Then, potassium cations can move through the membrane if four activation molecules are in their open state [11]. I_{leak}^{HH} is modeled as a regular ohmic current with constant conductance g_{leak}.

In our model, ion channel noise is introduced by means of Langevin sources in the equations governing the time evolution of the gating parameters $\gamma(t)$, with $\gamma(t)=m(t)$, $h(t)$ or $n(t)$. In the simulation, $\gamma(t)$ is updated every time step Δt following the HH model as [15]

$$\dot{\gamma}(t) = \alpha_\gamma(V_m)(1-\gamma) - \beta_\gamma(V_m)\gamma + \xi_\gamma(t), \tag{7}$$

where α_γ and β_γ are the voltage-dependent transition rates [11], and $\xi_\gamma(t)$ is the Langevin source of channel noise. Equation (7) is the Langevin generalization of the deterministic HH equations taking into account independent Gaussian white noise sources of vanishing mean, with autocorrelation function [15]

$$\langle \xi_\gamma(t)\xi_\gamma(t')\rangle = \frac{2}{\rho_{ion} S}\frac{\alpha_\gamma \beta_\gamma}{(\alpha_\gamma + \beta_\gamma)}\delta(t-t'), \tag{8}$$

where $\gamma = m$, h when ion = Na and $\gamma = n$ when $ion = K$. ρ_{ion} represents the ion channel densities, assumed as homogeneous, and S, the area of the membrane patch.

Ion shot noise is accounted for by means of a stochastic model in which the Monte Carlo technique is employed for the determination of the time of ion passage through the membrane following the HH equations [16–19]. The probabilities for the different ions to cross the cell membrane are considered to be independent of each other, and Gillespie

method [24, 25] is used to account for their stochastic transmembrane kinetics. The probability per unit time that a given ion crosses the membrane is calculated as [18]

$$P_{\text{ion}} = \left|I_{\text{ion}}^{\text{HH}}\right| S \Big/ e, \tag{9}$$

where e is the elementary charge. Assuming the crossing of ions through the membrane as a memoryless process, the time between crossing events is calculated following Poissonian statistics. The particular type of ion crossing the membrane is randomly determined according to the respective probabilities. The values of I_{ion}, calculated from the number of ions actually crossing the membrane during t, are then used in Eq. (1) to evaluate the new value of V_{m} for the next t and to calculate the total ion current density $\sum_{\text{ion}} I_{\text{ion}}$. Thus, I_{ion} and V_{m} contain the influence of the fluctuations associated with the random passage of ions through the cell membrane. All the details of this model and the values of the involved parameters can be found in Table 1. When ion shot noise is not included in the calculations, I_{ion} are evaluated as $I_{\text{ion}}^{\text{HH}}$ [Eqs. (2)–(4)].

The noise behavior of the system is studied in terms of the autocorrelation function $C_{V_{\text{m}}}(t)$ and spectral density $S_{V_{\text{m}}}(f)$ of the membrane voltage fluctuations. $S_{V_{\text{m}}}(f)$ is calculated from the Fourier transform of a V_{m} sequence of 300 s when the threshold condition is achieved by applying increasing values of I_{app} and 600 s when a similar situation is acquired by decreasing S.

We note that our model for the inclusion of shot noise considers, as a first approximation, that the passage of ions through the membrane is a Poissonian process, i.e., ions cross the membrane independently of each other. However, more rigorous studies of single open ion channels, performed by means of a coupled molecular dynamics/Monte Carlo approach with input parameters obtained from atomistic simulations, indicate the existence of correlations in ion motion within the channel [26, 27]. Such correlations may lead to values of the Fano factor higher than one, which means a level of noise higher than that of a Poissonian process, what would make shot noise even more relevant on membrane voltage dynamics than what found in our calculations.

Table 1 Values for the parameters involved in the HH model

Name	Value and unit	Description
C_{m}	1 μF cm^{-2}	Membrane capacitance
$g_{\text{Na}}^{\text{max}}$	120 mS cm^{-2}	Maximal gated sodium conductance
$g_{\text{K}}^{\text{max}}$	36 mS cm^{-2}	Maximal gated potassium conductance
g_{leak}	0.3 mS cm^{-2}	Leak conductance
V_{Na}	115 mV	Sodium reversal potential
V_{K}	−12 mV	Potassium reversal potential
V_{leak}	10.6 mV	Leak reversal potential
ρ_{Na}	60 μm^2	Sodium channel density
ρ_{K}	18 μm^2	Potassium channel density

3 Results and discussion

3.1 Influence of channel and shot noise separately

In order to illustrate the influence of the channel and shot noise sources, considered separately, on the V_{m} fluctuations with respect to the deterministic case (in the absence of any noise source), Fig. 1 presents (a) the time evolution of V_{m} and (b) $C_{V_{\text{m}}}(t)$, when considering an external excitation $I_{\text{app}} = 0.08$ Am^{-2} in a cell membrane of $S = 1000$ μm^2. This value of I_{app} leads to the appearance of a full train of spikes in $V_{\text{m}}(t)$ even in the absence of noise sources (Fig. 1a). In the deterministic case, the coefficient of variation CV defined as $\sqrt{\overline{T^2} - \overline{T}^2}/\overline{T}$ (where $\overline{T}$ and $\overline{T^2}$ are, respectively, the mean and the mean-squared values of interspike intervals), which represents a measure of the spike coherence [15], is zero due to the total regularity of the output signal. When ion shot noise is considered, CV is still around zero (3×10^{-3}), since the coherence is mostly preserved; however, $C_{V_{\text{m}}}(t)$ is slightly modified with respect to the deterministic case. In both cases, $C_{V_{\text{m}}}(t)$ is a periodic signal of period around 0.0167 s. On the contrary, channel noise, much more intense than shot noise, noticeably deteriorates the coherence. Due to this, CV = 1.54, clearly evidencing the lack of coherence, and $C_{V_{\text{m}}}(t)$ tends to zero in around 250 ms.

The corresponding $S_{V_{\text{m}}}(f)$ to the previous cases is shown in Fig. 2. $S_{V_{\text{m}}}(f)$ presents peaks at a characteristic spiking

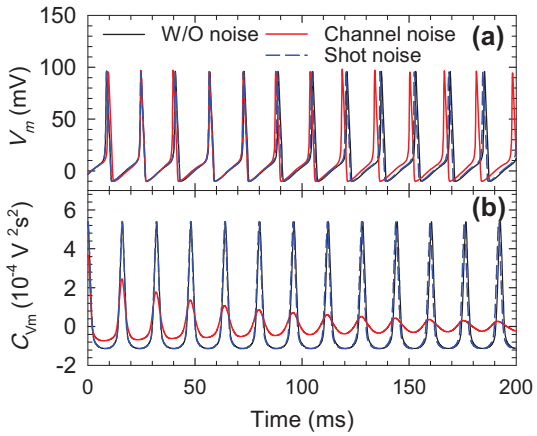

Fig. 1 **a** $V_{\text{m}}(t)$ and **b** $C_{V_{\text{m}}}(t)$ for $I_{\text{app}} = 0.08$ Am^{-2} when no noise source is taken into account in the system and in the cases in which channel or shot noise is considered separately. $S = 1000$ μm^2

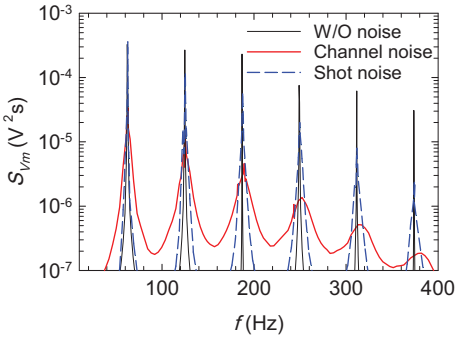

Fig. 2 $S_{V_m}(f)$ for $I_{app}=0.08$ Am^{-2} when no noise source is taken into account in the system and in the cases in which channel or shot noise is considered separately. $S=1000$ μm^2

frequency around 60 Hz [15, 17, 19] and its harmonics. In the deterministic case, the δ-like peaks further indicate the coherence inherent to the regular spiking. Shot noise slightly modifies $S_{V_m}(f)$ with respect to the deterministic case, but, as mentioned, the coherence is essentially preserved. In contrast, in the presence of channel noise, peaks in $S_{V_m}(f)$ are less pronounced and cover a wider frequency range around the characteristic frequency and its harmonics, again indicating the loss of coherence.

3.2 Interplay in the presence of an external excitation

In order to analyze the influence of channel and shot noise on the spiking activity at the onset of instabilities, we consider a membrane patch $S=1000$ μm^2, for which both noise sources are insufficient for the activation of spikes in the absence of external excitation, and the limit of threshold conditions is reached by applying increasing values of I_{app}. To illustrate this point, sequences of the time evolution of V_m are plotted in Fig. 3 for different external constant currents when only ion channel noise is considered in the system. The excitation $I_{app}=0.04$ Am^{-2} is still weak for the onset of spikes; however, the fluctuations in $V_m(t)$ are stronger than for $I_{app}=0$ Am^{-2}. An increasing number of spikes arise from a threshold value of I_{app} around 0.045 Am^{-2}. Values of I_{app} around 0.06 Am^{-2} lead to the appearance of random spikes which are absent in the deterministic case. Interestingly, for the larger external excitations, as in the case of 0.07 Am^{-2} and 0.08 Am^{-2}, instead of random isolated spikes, channel noise originates or deletes entire spike trains of different time length. This could be at the origin of the large values obtained for *CV*.

To clarify the influence of the noise sources in the spiking activity, Fig. 4a exhibits, as a function of I_{app}, the mean value of V_m, $\overline{V}_m$, when the excitation current is not enough for the emergence of spikes, and the number of spikes occurring

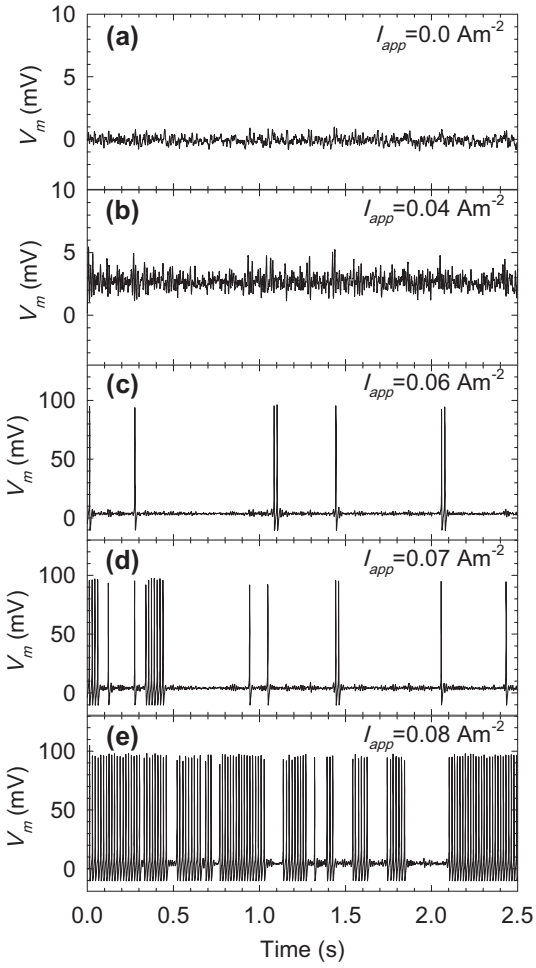

Fig. 3 $V_m(t)$ for **a** $I_{app}=0.0$ Am^{-2}, **b** $I_{app}=0.04$ Am^{-2}, **c** $I_{app}=0.06$ Am^{-2}, **d** 0 $I_{app}=0.07$ Am^{-2} and **e** $I_{app}=0.08$ Am^{-2}, when ion channel noise is taken into account in the system. $S=1000$ μm^2

in a simulation time of 300 s in the deterministic case and when channel noise and shot noise are taken into account. In real biological systems, V_m is around −68 mV in the absence of I_{app}; this is the so-called resting voltage. However, the HH model considers $V_m=0$ as resting voltage for simplicity. When injecting external constant currents of values ranging from 0 to about 0.05 Am^{-2}, no spikes appear, but new resting conditions take place, with $\overline{V}_m$ covering from zero to almost 4 mV as I_{app} increases and V_m remaining as a stable holding voltage [12]. For a given I_{app}, $\overline{V}_m$ takes similar values in the absence of noise sources, considering only channel noise and considering both channel noise and shot noise (not represented in the figure). As expected, a spike train abruptly emerges in the deterministic case, being the threshold value of around 0.065 Am^{-2}. For higher values of I_{app}, the number of spikes very slightly increases ($I_{app}=0.07$ Am^{-2} and 0.08 Am^{-2}) due to the shorter interspike interval because of the higher I_{app}. In contrast, when channel noise is considered, the onset of voltage spikes takes place for lower values

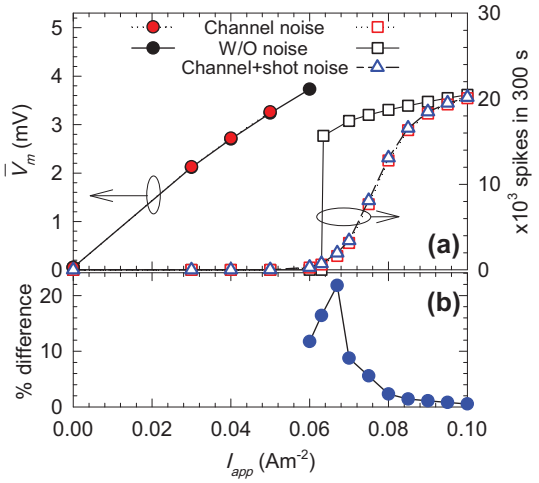

Fig. 4 **a** Mean value of V_m in the absence of spikes and the number of spikes occurring in a simulation time of 300 s as a function of I_{app} in the deterministic case, when channel noise is considered and when also shot noise is taken into account. **b** Percentage of spikes added by the inclusion of shot noise with respect to the case in which only channel noise is considered. $S = 1000\ \mu m^2$

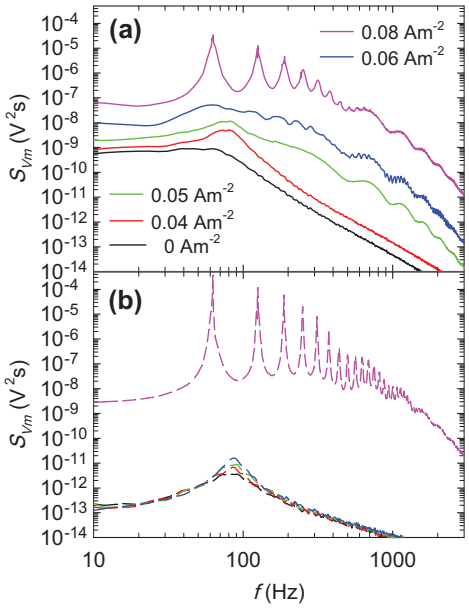

Fig. 5 $S_{V_m}(f)$ for different values of I_{app} when **a** ion channel noise and **b** ion shot noise are taken into account separately in the system. $S = 1000\ \mu m^2$

of I_{app}, around 0.055 Am^{-2}, since for high enough values of I_{app} the noise assists their appearance. In contrast, above threshold conditions, noise suppresses a significant amount of spikes with respect to the deterministic case. Noticeably, the interplay between channel and shot noise leads to the appearance of slightly higher number of spikes than when channel noise is considered alone. This behavior is further illustrated in Fig. 4b, which shows the percentage of spikes added by the inclusion of shot noise with respect to the case in which only channel noise is considered. The maximum difference is achieved for around $I_{app} = 0.067$ Am^{-2}, just above the threshold in the deterministic case. Ion shot noise always adds extra spikes when considered together with channel noise. As expected, when the excitation is large enough, the number of spikes is not influenced by the presence or absence of any type of noise.

Figure 5 presents $S_{V_m}(f)$ when (a) ion channel noise and (b) ion shot noise are considered separately in the simulations, for I_{app} ranging from 0 to 0.08 Am^{-2}, covering the subthreshold regime and the onset of oscillations. For $I_{app} = 0$ Am^{-2} and 0.04 Am^{-2}, ion channel noise is not strong enough for the onset of spiking (Fig. 4). For 0.04 Am^{-2}, channel noise is responsible for a peak in $S_{V_m}(f)$ at around 80–90 Hz, evidencing a rhythm in the $V_m(t)$ fluctuations related to the internal dynamics of the system [28]. This frequency behavior of the V_m fluctuations originated by channel noise has been also reported in Refs. [12, 14]. When $I_{app} = 0.05$ Am^{-2}, still insufficient for the onset of spike trains but close to their appearance, $S_{V_m}(f)$ exhibits a remarkable increase in the whole frequency range [19, 28]. This change in the noise behavior, typical at the onset of instabilities, has been observed in other physical systems, like electronic devices [29]. For $I_{app} = 0.08$ Am^{-2}, when full trains of voltage spikes of different time length are achieved (Fig. 3), $S_{V_m}(f)$ presents peaks around the characteristic spiking frequency and its harmonics.

In the case of considering only ion shot noise in the simulations (Fig. 5b), the values of $S_{V_m}(f)$ in the subthreshold regime are around four orders of magnitude lower than those obtained when channel noise is the only noise source considered. $S_{V_m}(f)$, as occurs in the case of considering channel noise, exhibits a peak at about 80–90 Hz in the absence of external excitation and for the lower values of I_{app}. This maximum reveals the existence of intrinsic rhythmic oscillations in the time evolution of V_m due to ion shot noise even for large values of S, for which this noise source is extremely weak [17]. In contrast to the gradual increase in the values of $S_{V_m}(f)$ when increasing I_{app} in the presence of channel noise, ion shot noise leads to similar values of $S_{V_m}(f)$ for different I_{app} as long as the system remains in subthreshold regime and then suddenly increases beyond the threshold value (in the figure, $I_{app} = 0.08$ Am^{-2}) when a full spike train is triggered. Under this condition, shot noise does not significantly modify the values of $S_{V_m}(f)$ with respect to the deterministic case (Fig. 2).

To illustrate the interplay between channel and shot noise at the onset of spiking activity, Fig. 6 shows $S_{V_m}(f)$ when a cell membrane of $S = 1000\ \mu m^2$ is excited with different constant values of I_{app}, both when channel noise is the only noise source considered in the system and in the

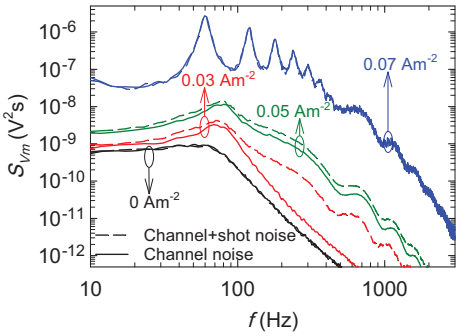

Fig. 6 $S_{V_m}(f)$ for different values of I_{app} when channel noise is the only noise source considered in the system and in the case in which also shot noise is taken into account. S = 1000 μm^2

case in which also shot noise is taken into account. In the absence of excitation, both cases practically coincide, thus evidencing the expected negligible influence of shot noise. For $I_{app} = 0.07$ Am^{-2}, high enough for generation of spikes, the peaks in $S_{V_m}(f)$ denote their presence and both cases again essentially overlap. However, due to the extra spikes originated by shot noise, the maximum value of $S_{V_m}(f)$, appearing at the characteristic frequency and its harmonics, is always higher than the one due to only channel noise. The respective values of S_{V_m} at the characteristic frequency are 3.75×10^{-6} V^{2}s and 3.32×10^{-6} V^{2}s (hardly noticeable in the figure), thus being the difference 11.5%.

When I_{app} is 0.03 Am^{-2}, still insufficient for the onset of spikes but close to their appearance, the spectral density exhibits a significant increase when ion shot noise is included in the simulation with respect to case in which channel noise is the only source considered. The characteristic shape that acts as a prelude of the spiking activity is strengthened by the presence of shot noise. The difference between both cases can be observed up to 0.05 Am^{-2}. Remarkably, we can conclude that shot noise plays a role in the noise behavior by the interplay with channel noise, particularly at the onset of the spiking activity, and reinforced by the onset of spikes in form of trains.

Given that the surface of the membrane patch determines the intensity of both channel noise and shot noise, we have performed the previous analysis for other values of S. The qualitative behavior of S_{V_m} is very similar to that found for $S = 1000$ μm^2 as long as S is large enough, so that the appearance of spontaneous spikes due to noise does not take place in the absence of external excitation, i.e., $S > 150$ μm^2 (see Fig. 8 in next Sect. 3.3). As one could expect, the main observed difference is that for decreasing values of S, the onset of spikes occurs for lower values of I_{app}. Thus, the previously illustrated behavior in S_{V_m} due to the interplay between channel and shot noise is visible for smaller values of I_{app}. For example, we have verified that for $S = 500$ μm^2, S_{V_m} exhibits the described behavior for I_{app} around

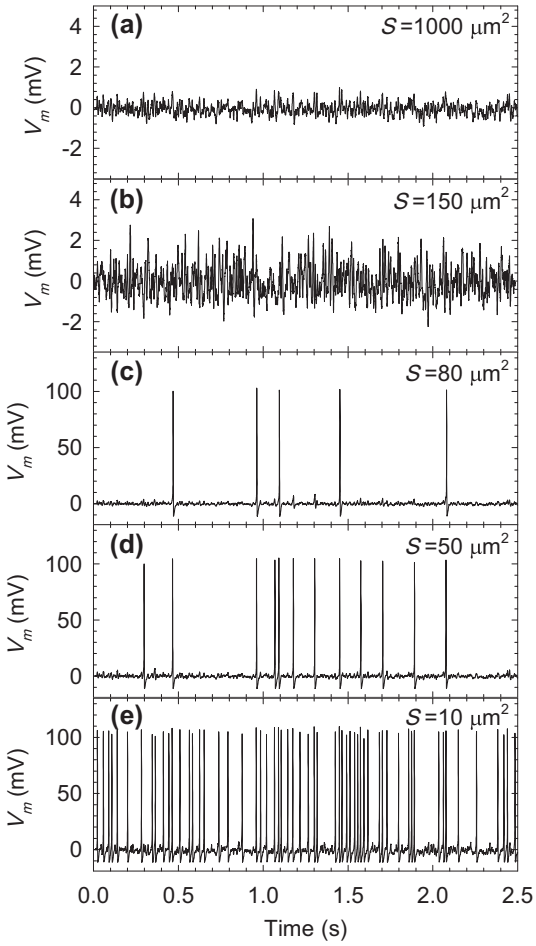

Fig. 7 $V_m(t)$ for **a** $S = 1000$ μm^2, **b** $S = 120$ μm^2, **c** $S = 80$ μm^2, **d** $S = 50$ μm^2 and **e** $S = 10$ μm^2, when ion channel noise is taken into account in the system. $I_{app} = 0$ Am^{-2}

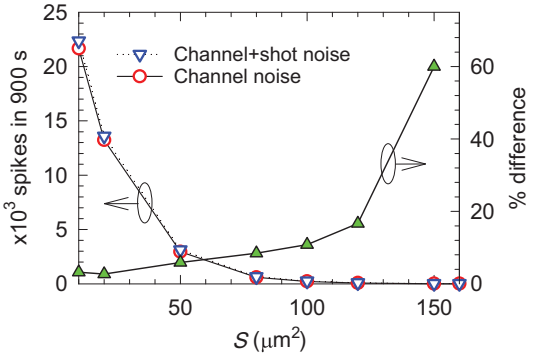

Fig. 8 Number of spikes occurring in a simulation time of 900 s as a function of S when channel noise is considered and when also shot noise is taken into account, and percentage of spikes added by the inclusion of shot noise with respect to the case in which only channel noise is considered. $I_{app} = 0$ Am^{-2}

0.025 Am^{-2}, and it is still noticeable for $I_{app}=0.03$ Am^{-2}. On the other hand, for $S=1500$ μm^2, the interplay starts being visible for I_{app} around 0.05 Am^{-2}, higher current than for $S=1000$ μm^2, and the difference observed between the cases with the presence and absence of shot noise is smaller.

3.3 Interplay in the absence of an external excitation

In the absence of excitation, the onset of voltage spikes can be achieved by reducing S, since the strength of both ion channel noise and ion shot noise increases, leading to the appearance of spontaneous spikes in the biological membrane [15]. However, the scenario is different than when applying a nonzero I_{app}, since random individual spikes, instead of trains of spikes, are originated or suppressed by the influence of noise sources. To illustrate this behavior, Fig. 7 shows sequences of the time evolution of V_m for different S decreasing from 1000 μm^2 to 10 μm^2 in the presence of channel noise. For $S>150$ μm^2, apart from spurious spontaneous voltage spikes, the system essentially remains in subthreshold conditions; nevertheless, when decreasing S, intrinsic rhythmic oscillations of higher amplitude are noticeable in the time evolution of V_m. Numerous random spikes appear for $S<80$ μm^2, and, as expected, the number of spikes increases when reducing S. In contrast with the case of reaching the threshold by applying an external current in a large membrane patch, in which spike trains are originated or suppressed by the presence of noise, here an increasing number of spontaneous individual spikes are originated when diminishing S.

The number of spikes as a function of S occurred during a simulation time of 900 s is shown in Fig. 8 when channel noise is the only noise source considered in the simulations and when shot noise is additionally taken into account. For clarity, the percentage of difference between both situations is also plotted. For S around 150 μm^2, the increasing joint action of channel and shot noise leads to the emergence of spontaneous spikes that are absent when channel noise in the only noise source considered in the simulations. For $S<150$ μm^2, shot noise is responsible for the appearance of additional spikes via the interplay with channel noise. The difference with respect to the case in which channel noise is the only noise source considered is higher at the surface values around which the onset of spikes takes place, and then, it decreases for lower S.

Figure 9 shows $S_{V_m}(f)$ for different values of S ranging from 1000 to 50 μm^2, thus including a non-spiking regime and the onset of spiking activity, when channel noise is the only noise source considered in the system and in the case in which also shot noise is taken into account. For $S>150$ μm^2, when the noise is not sufficient for the onset of spikes, and for $S<100$ μm^2, when the noise is strong and numerous

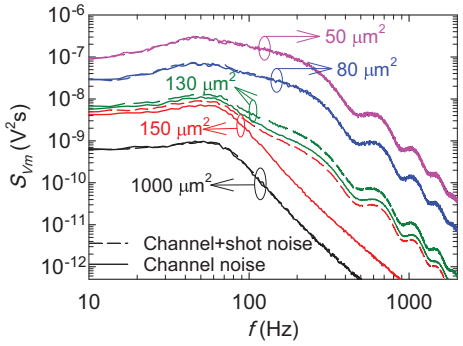

Fig. 9 $S_{V_m}(f)$ for different values of S in the absence of external excitation when channel noise is the only noise source considered in the system and in the case in which also shot noise is taken into account. $I_{app}=0$ Am^{-2}

spikes randomly appear in the cell membrane, both cases coincide, thus evidencing the expected negligible influence of shot noise. However, for S about 150 μm^2, around the onset of spikes, the interplay between both channel and shot noise sources displays a visible influence over the case in which channel noise is the only noise source considered. This is linked to the mentioned change on the noise behavior that typically occurs at the onset of instabilities. The influence of shot noise in the global noise behavior is also visible when decreasing S at least up to 130 μm^2. These results further demonstrate the significant role played by shot noise at the onset of instabilities by means of the interplay with channel noise.

To complete this analysis, we have considered cases in which the intensity of shot noise is artificially modified [17]. As expected, when the intensity is increased, the influence of shot noise is more visible in $S_{V_m}(f)$, always in the case of $S\sim150$ μm^2. Remarkably, in the opposite case, we have verified that the signature of shot noise is still visible when the intensity of shot noise is artificially diminished up to a factor ~0.25.

4 Conclusions

Subthreshold voltage fluctuations in neural membranes modeled by means of the HH model have been studied in terms of $S_{V_m}(f)$ when considering ion channel noise and ion shot noise sources in the system. In the model, ion channel noise is included by means of Langevin sources and ion shot noise is considered in terms of the probabilities for different ions to cross the cell membrane. The spiking activity has been reached by applying increasing values of I_{app} in a large membrane patch and by reducing S in the absence of external excitation. In both cases, at the onset of instabilities and around threshold conditions, the signature of shot

noise is significantly visible when combined with channel noise, while its influence is otherwise negligible as typically predicted.

When a nonzero external current is considered, noise is at the origin of the onset or suppression of random spike trains; thus, the influence of shot noise in the spectral density is very significant when considered together with channel noise in the simulations. In contrast, when decreasing the value of S to achieve similar conditions, noise is at the origin of the onset or suppression of random spontaneous individual spikes. However, the influence of shot noise is still visible in the noise behavior of the system, since extra spikes are provided by the interplay with channel noise when S is around the onset of spontaneous spikes.

References

1. Eisenberg, B.: Ion channels as devices. J. Comput. Electron. **2**, 245–249 (2003)
2. Ha, S.D., Ramanathan, S.: Adaptive oxide electronics: a review. J. Appl. Phys. **110**, 071101 (2011)
3. Kaneko, Y., Nishitani, Y., Ueda, M.: Ferroelectric artificial synapses for recognition of a multishaded image. IEEE Trans. Electron. Dev. **61**, 2827–2833 (2014)
4. Prezioso, M., Merrikh-Bayat, F., Hoskins, B.D., Adam, G.C., Likharev, K.K., Strukov, D.B.: Training and operation of an integrated neuromorphic network based on metal-oxide memristors. Nature **512**, 61–64 (2015)
5. Romeo, A., Dimonte, A., Tarabella, G., D'Angelo, P., Erokhin, V., Iannotta, S.: A bio-inspired memory device based on interfacing physarum polycephalum with an organic semiconductor. APL Mater. **3**, 014909 (2015)
6. Faisal, A.A., Selen, L.P.J., Wolpert, D.M.: Noise in the nervous system. Nat. Rev. **9**, 292–303 (2008)
7. Kilinc, D., Demir, A.: Noise in neuronal and electronic circuits: a general modeling framework and non-Monte Carlo simulation techniques. IEEE Trans. Biomed. Circuits Syst. **11**, 958–974 (2017)
8. Kilinc, D., Demir, A.: Spike timing precision of neuronal circuits. J. Comput. Neurosci. **44**, 341–362 (2018)
9. Chein, W.R., Midtgaard, J., Shepherd, G.M.: Forward and backward propagation of dendritic impulses and their synaptic control in mitral cells. Science **278**, 463–467 (1997)
10. Chua, L.: Memristor, Hodgkin–Huxley and edge of chaos. IOP Nanotechnol. **24**, 383001 (2013)
11. Hodgkin, L.A., Huxley, A.F.: A quantitative description of membrane current and its application to conduction and excitation in nerve. J. Physiol. **117**(4), 500–544 (1952)
12. Steinmetz, P.N., Manwani, A., Koch, C.: Subthreshold voltage noise due to channel fluctuations in active neuronal membranes. J. Comput. Neurosci. **9**, 113–148 (2000)
13. Jacobson, G.A., Diba, K., Yaron-Jakoubovitch, A., Oz, Y., Koch, C., Segev, I., Yaron, Y.: Subthreshold voltage noise of rat neocortical pyramidal neurones. J. Physiol. **564**, 145–160 (2005)
14. Linaro, D., Storace, M., Giugliano, M.: Accurate and fast simulation of channel noise in conductance-based model neurons by diffusion approximation. Plos Comput. Biol. **7**, e1001102 (2011)
15. Schmid, G., Goychuk, I., Hänggi, P.: Stochastic resonance as a collective property of ion channel assemblies. Europhys. Lett. **56**, 22–28 (2001)
16. Vasallo, B.G., Pardo-Galán, F., Mateos, J., González, T., Hedayat, S., Hoel, V., Cappy, A.: Stochastic model for action potential simulation including ion shot noise. J. Comput. Electron. **16**, 419–430 (2017)
17. Vasallo, B.G., Mateos, J., González, T.: Ion shot noise in Hodgkin and Huxley neurons. J. Comput. Electron. **17**, 1790–1796 (2018)
18. Vasallo, B.G., Mateos, J., González, T.: Stochastic model for ion shot noise in Hodgkin and Huxley neurons. In: IEEE Proceedings of International Conference on Noise and Fluctuations (ICNF), 2017. DOI: 10.1109/icnf.2017.7985975 (2017)
19. Vasallo, B.G., Mateos, J., González, T.: Interplay between channel and shot noise in subthreshold voltage fluctuations of neural membranes. In: Proceedings of International Conference on Noise and Fluctuations (ICNF), 2019. DOI: 10.5075/epfl-ICLAB-ICNF-269293 (2019)
20. Schmid, G., Goychuk, I., Hänggi, P.: Channel noise and synchronization in excitable membranes. Phys. A **325**, 165–175 (2003)
21. Schmid, G., Goychuk, I., Hänggi, P., Zeng, S., Jung, P.: Effect of channel block on the spiking activity of excitable membranes in a stochastic Hodgkin–Huxley model. Phys. Biol. **1**, 61–66 (2004)
22. Adair, R.K.: Noise and stochastic resonance in voltage-gated ion channels. PNAS **100**, 12099–12104 (2003)
23. Faisal, A.A., White, J.A., Laughlin, S.B.: Ion-channel noise places limits on the miniaturization of the brain's wiring. Curr. Biol. **15**, 1143–1149 (2005)
24. Gillespie, D.T.: A general method for numerically simulating the stochastic time evolutions of coupled chemical reactions. J. Comput. Phys. **22**, 403–434 (1976)
25. Gillespie, D.T.: Exact stochastic simulation of coupled chemical reactions. J. Phys. Chem. **81**, 2340–2361 (1977)
26. Brunetti, R., Affinito, F., Jacoboni, C., Piccinini, E., Rudan, M.: Shot noise in single open ion channels: a computational approach based on atomistic simulations. J. Comput. Electron. **6**, 391–394 (2007)
27. Piccinini, E., Affinito, F., Brunetti, R., Jacoboni, C., Rudan, M.: Computational analysis of current and noise properties of a single open ion channel. J. Chem. Theory Comput. **3**, 248–255 (2007)
28. Kuang, S., Wang, J., Zeng, T.: Intrinsic rhythmic fluctuation of membrane voltage evoked by membrane noise in the Hodgkin–Huxley system. Acta Phys. Pol. A **117**, 435–438 (2010)
29. García-Pérez, O., Alimi, Y., Song, A., Íñiguez-de-la-Torre, I., Pérez, S., Mateos, J., González, T.: Experimental assessment of anomalous low-frequency noise increase at the onset of Gunn oscillations in InGaAs planar diodes. Appl. Phys. Lett. **105**(1–4), 113502 (2014)